Electronic Supplementary Material (ESI) for Physical Chemistry Chemical Physics

Supplementary Material (ESI) for PCCP

Electronic Supplementary Information

Faster Nucleation at Lower pH: Amorphous Phase Mediated Nucleation Kinetics

Shuqin Jiang,[a,b] *Yan Chen,*[a,b] *Haihua Pan,*[*a] *Yinjia Zhang,*[b] *Ruikang Tang*[*b]

[a] *Qiushi Academy for Advanced Studies, Zhejiang University, Hangzhou 310027, China. E-mail: panhh@zju.edu.cn*

[b]*Department of Chemistry, and Centre for Biomaterials and Biopathways, Zhejiang University, Hangzhou 310027, China. E-mail: rtang@zju.edu.cn*

Experiments

Materials:

All of the chemicals used in this study were of analytical grade and were purchased from Aladdin Reagent (Shanghai, China) unless specifically mentioned. Triple distilled water was used.

Crystallization kinetics:

Calcium solutions contained $CaCl_2$ and $MgCl_2$, and phosphate solutions contained Na_2HPO_4, Na_2SO_4, NaCl, KCl, N-2-hydroxyethylpiperaz- ine-N-2'-ethanesulfonic acid, (HEPES, Genom BioMed Technology Inc., Hangzhou, China). All working solutions were prepared from concentrated stock solutions. For stock solutions preparations, the salts were dissolved with designated amount of water and stored overnight. All solutions were filtered through 0.22 µm Millipore films prior to use. All experiments were conducted at temperature of 37.0±0.5°C. The *p*H values of calcium and phosphate solutions were pre-adjusted to designated value by 1.0 M NaOH, which was prepared for one week. The SBF solutions were obtained by rapid mixing of equal volumes of designated calcium and phosphate solutions, and the concentrations of each species were list in Tables S1 and S2 in Supporting Information. The *p*H curve of each solution was monitored by a PHSJ-3F *p*H meter and an E-201-C c-omposite electrode (Leici Instrument, Shanghai, China). The *p*H electrodes were calibrated by 25 mM NaH_2PO_4/Na_2HPO_4 standard buffer solution (pH = 6.86, 25 °C) and 10mM $Na_2B_4O_7{\cdot}10H_2O$ standard buffer solution (pH = 9.18, 25 °C) with an average error less than 0.02 *p*H units. The induction times are determined by the intersections of tangents over the initially flat levels of *p*H (stage I) and over the subsequent fast *p*H drop during the precipitation of apatite (stage II) (cf. Figure 1a). After reaction for 3 hrs, the precipitation were centrifuged (Eppendorf model 5418), wash with ethanol for three times, dried at 300 °C for 1hr, and weighted. The yields of crystallization were calculated by the theoretical amount of solid (calculated by VMINTEQ 3.0[s1])

Characterization:

At designated times, the suspension were removed and centrifuged at 10,000 g for 2 min, and washed with ethanol for three times. The mineral phase and crystallinity were characterized by FITR (Thermo-Nicolet Nexus 670) and XRD (Rigaku D/MAX-2550pc). For TEM examination, the samples were obtained by paddling copper grid in suspension, and washing with water and ethanol, and lamp-light dried. Dark field TEM and High Resolution TEM observations were performed by a Philips CM200 at the accelerating voltage of 160 KV.

Solution Chemistry Calculation:

The supersaturations of the solutions were calculated by VMINTEQ 3.0. Davies approximation of the Debye–Hückel equation was used for calculating the activity coefficients (parameter b = 0.3 is applied). The solubility product, K_{SP}, of HAP (pKsp = 58.33, MINTEQ database: NIST 46.7), and ACP (pKsp= 25.5[s2-s4]) were used in calculation.

Titration of HEPES-Phosphate solutions

The buffer capacities of effective solutions (after the precipitation of ACP) were measured by titration with 0.5 M HCl in 10 mL of buffer solutions. The compositions of HEPES-Phosphate Buffer solutions were given as following: The compositions and concentrations of buffer solution were the same with Table S1 except that calcium was removed from solution to prevent the possible precipitation during solution preparation and titration; phosphate concentration was set to the effective phosphate concentration (ie. after the precipitation of ACP, $[P]_{eff} = [P]_0 - 2*C_{ACP}$, $[P]_0$ =10mM) (C_{ACP} is given in Table 1) As at later stage of crystallization, most of phosphate will be consumed, the buffer capacity for solutions without phosphate were also titrated.

The results show that *p*H drops faster at lower *p*H conditions (see Fig. S4). When phosphate is removed from system, the buffer capacity is reduced as well, especially for *p*H 6.8, which can explain the faster drop of *p*H as HAP formation (Fig. 1).

Notes and References

S1. J.P. Gustafsson, 2010. Visual MINTEQ, Version 3.0, Stockholm. Available from: http://www.lwr.kth.se/English/OurSoftware/vminteq.

S2. M. R. Christoffersen, J. Christoffersen, and W. Kibalczyc, *J. Cryst. Growth*, 1990, **106**, 349.

S3. S. V. Dorozhkin and M. Epple, *Angew. Chem. Int. Ed.*, 2002, **41**, 3130.

S4. As the morphology of ACP found in this work is analogues to that of ACP1 in ref S2, pKsp=25.5 is applied. We find that the appling of other values from ref. S2-S3 did not change the relationship that the nucleation rate is proportional to $\{Ca\}^2_{eff}\, C_{ACP}$.

Tables

Table S1. The composition of 10 mM $CaCl_2$ 6 mM Na_2HPO_4 solutions. The initial *p*H of the solutions (from 6.8 to 7.6) is adjusted with 1.0 M NaOH solution.

Ion.	Na^+	K^+	Mg^{2+}	Cl^-	SO_4^{2-}	Ca^{2+}	PO_4^{3-}	$HEPES^-$
C/mM	133.0	5.0	1.5	148.0	0.5	10.0	6.0	10.0

Table S2. The composition of solutions with different calcium/phosphate concentrations at given *p*H conditions (Note: the activity ratio of {Ca}/{P} are kept at 1.67, see Table S3)

***p*H=6.8**

Ion. C/(mM)	No.				
	1.	2.	3.	4.	5.
H^+	15.0	16.0	17.0	19.7	23.9
Na^+	131.0	129.0	127.4	122.6	115.8
K^+	5.0	5.0	5.0	5.0	5.0
Mg^{2+}	1.5	1.5	1.5	1.5	1.5
Cl^-	148.0	148.0	148.0	148.0	148.0
SO_4^{2-}	0.5	0.5	0.5	0.5	0.5
Ca^{2+}	10.0	12.0	13.8	18.9	26.5
PO_4^{3-}	5.0	6.0	7.0	9.7	13.9
$HEPES^-$	10.0	10.0	10.0	10.0	10.0
ln(*S*)	27.13	28.43	29.46	31.65	33.97

***p*H=7.0**

Ion. C/(mM)	No.				
	1.	2.	3.	4.	5.
H^+	14.4	15.8	17.8	19.4	24.0
Na^+	134.2	132.2	129.6	127.4	121.6
K^+	5.0	5.0	5.0	5.0	5.0
Mg^{2+}	1.5	1.5	1.5	1.5	1.5
Cl^-	148.0	148.0	148.0	148.0	148.0
SO_4^{2-}	0.5	0.5	0.5	0.5	0.5
Ca^{2+}	7.8	10.2	13.5	16.2	23.7
PO_4^{3-}	4.4	5.8	7.8	9.4	14.0
$HEPES^-$	10.0	10.0	10.0	10.0	10.0
ln(*S*)	27.87	29.82	31.82	33.08	35.65

pH=7.2

Ion. C/(mM)	No.				
	1.	2.	3.	4.	5.
H^+	14.5	16.2	17.5	21.0	28.0
Na^+	135.9	134.2	132.8	129.4	123.0
K^+	5.0	5.0	5.0	5.0	5.0
Mg^{2+}	1.5	1.5	1.5	1.5	1.5
Cl^-	148.0	148.0	148.0	148.0	148.0
SO_4^{2-}	0.5	0.5	0.5	0.5	0.5
Ca^{2+}	7.05	9.6	11.6	16.8	27.0
PO_4^{3-}	4.5	6.2	7.5	11.0	18.0
$HEPES^-$	10.0	10.0	10.0	10.0	10.0
ln(S)	29.57	31.80	33.11	35.65	38.75

pH=7.4

Ion. C/(mM)	No.				
	1.	2.	3.	4.	5.
H^+	15.0	16.0	19.0	25.0	30.0
Na^+	137.0	136.2	134.0	129.8	126.4
K^+	5.0	5.0	5.0	5.0	5.0
Mg^{2+}	1.5	1.5	1.5	1.5	1.5
Cl^-	148.0	148.0	148.0	148.0	148.0
SO_4^{2-}	0.5	0.5	0.5	0.5	0.5
Ca^{2+}	7.0	8.4	12.5	20.6	27.3
PO_4^{3-}	5.0	6.0	9.0	15.0	20.0
$HEPES^-$	10.0	10.0	10.0	10.0	10.0
ln(S)	31.81	33.09	35.84	39.13	40.91

pH=7.6

Ion. C/(mM)	No.				
	1.	2.	3.	4.	5.
H^+	14.0	14.8	16.9	21.6	25.6
Na^+	138.6	138.2	137.0	134.6	132.6
K^+	5.0	5.0	5.0	5.0	5.0
Mg^{2+}	1.5	1.5	1.5	1.5	1.5
Cl^-	148.0	148.0	148.0	148.0	148.0
SO_4^{2-}	0.5	0.5	0.5	0.5	0.5
Ca^{2+}	5.2	6.2	8.9	14.8	19.8
PO_4^{3-}	4.0	4.8	6.9	11.6	15.6
$HEPES^-$	10.0	10.0	10.0	10.0	10.0
ln(S)	31.79	33.06	35.59	39.00	40.87

Table S3. The activity of calcium {Ca}(mM) , phosphate {P} (mM) ({P}={H_3PO_4}+{$H_2PO_4^-$}+{HPO_4^{2-}}+{PO_4^{3-}}) , the supersaturation (*S*) of HAP before (*S*) and after the precipitation of ACP (S_{eff}), and the amount of ACP precipitated (C_{ACP}, mM) at different initial *p*H conditions, and calcium/phosphate concentrations.

***p*H=6.8**

No.	ln (S)	{Ca}	{P}	$\{Ca\}_{eff}$	$\{P\}_{eff}$	ln (S_{eff})	C_{ACP}
1.	27.13	2.603	1.563	1.931	1.014	24.33	0.945
2.	28.43	3.074	1.831	2.005	0.958	24.35	1.529
3.	29.46	3.482	2.093	2.050	0.926	24.35	2.079
4.	31.65	4.593	2.749	2.221	0.822	24.40	3.589
5.	33.97	6.125	3.677	2.454	0.707	24.44	5.864

***p*H=7.0**

No.	ln (S)	{Ca}	{P}	$\{Ca\}_{eff}$	$\{P\}_{eff}$	ln (S_{eff})	C_{ACP}
1.	27.87	2.033	1.214	1.400	0.766	24.62	0.872
2.	29.82	2.592	1.547	1.440	0.735	24.64	1.629
3.	31.82	3.321	1.995	1.481	0.705	24.65	2.685
4.	33.08	3.892	2.329	1.524	0.675	24.67	3.538
5.	35.65	5.364	3.213	1.614	0.619	24.70	5.942

***p*H=7.2**

No.	ln (S)	{Ca}	{P}	$\{Ca\}_{eff}$	$\{P\}_{eff}$	ln (S_{eff})	C_{ACP}
1.	29.57	1.817	1.085	1.028	0.599	24.93	1.084
2.	31.80	2.395	1.437	1.026	0.600	24.93	1.937
3.	33.11	2.829	1.690	1.031	0.595	24.93	2.599
4.	35.65	3.881	2.322	1.022	0.603	24.93	4.346
5.	38.75	5.716	3.424	0.981	0.642	24.91	7.798

***p*H=7.4**

No.	ln (S)	{Ca}	{P}	$\{Ca\}_{eff}$	$\{P\}_{eff}$	ln (S_{eff})	C_{ACP}
1.	31.81	1.768	1.061	0.744	0.503	25.23	1.416
2.	33.09	2.079	1.244	0.733	0.514	25.23	1.895
3.	35.84	2.930	1.754	0.692	0.560	25.20	3.309
4.	39.13	4.423	2.647	0.613	0.672	25.14	6.101
5.	40.91	5.524	3.301	0.555	0.781	25.08	8.400

***p*H=7.6**

No.	ln (S)	{Ca}	{P}	$\{Ca\}_{eff}$	$\{P\}_{eff}$	ln (S_{eff})	C_{ACP}
1.	31.79	1.330	0.790	0.567	0.411	25.56	1.034
2.	33.06	1.556	0.929	0.548	0.432	25.54	1.389
3.	35.59	2.136	1.272	0.510	0.481	25.51	2.332
4.	39.00	3.268	1.957	0.432	0.618	25.42	4.388
5.	40.87	4.126	2.473	0.380	0.747	25.35	6.112

Table S4. The effective activities of inorganic ions in 10 mM $CaCl_2$ 6 mM Na_2HPO_4 solutions at different *p*H conditions after the precipitation of ACP.

Effective activity (mM)	*p*H				
	6.8	7.0	7.2	7.4	7.6
$\{Na^+\}$	96.04	96.24	96.40	96.52	96.62
$\{K^+\}$	3.610	3.617	3.621	3.625	3.627
$\{Mg^{2+}\}$	0.375	0.379	0.383	0.386	0.389
$\{Cl^-\}$	107.3	107.5	107.6	107.7	107.8
$\{SO_4^{2-}\}$	0.115	0.117	0.119	0.121	0.122
$\{Ca^{2+}\}$	1.726	1.373	1.115	0.924	0.778
$\{PO_4^{3-}\}$	1.191E-6	1.689E-6	2.292E-6	3.041E-6	3.935E-6

Figures

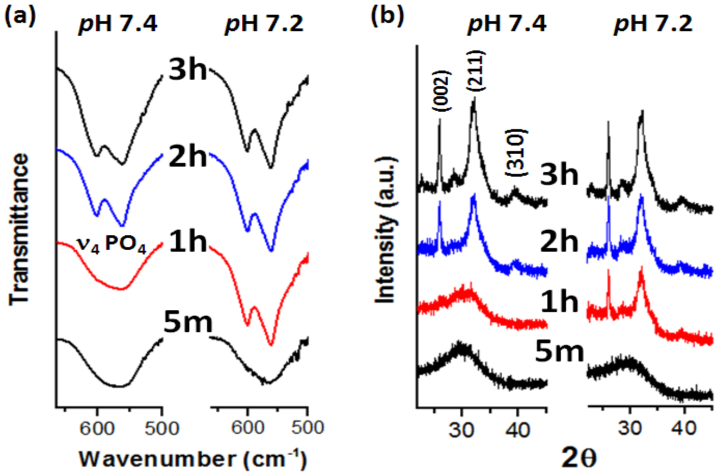

Figure S1. FTIR spectrums (a) and XRD patterns (b) of the mineral during the mineralization at initial pH of 7.4 (left) and 7.2 (right) at different time.

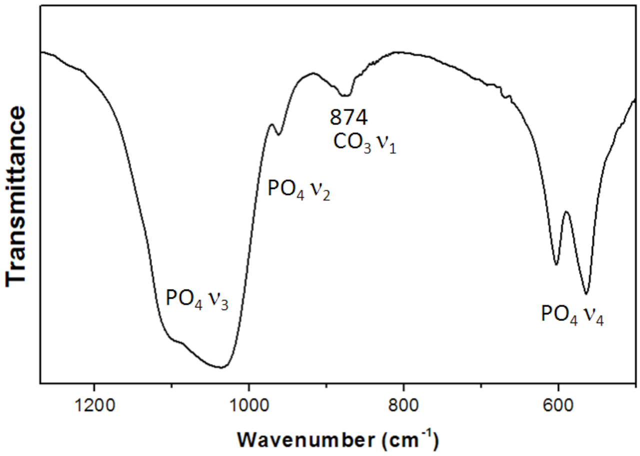

Figure S2. FTIR spectrum of the final minerals at 3 h proves that the apatite is carbonated hydroxyapatite, the analogous of biological apatite in bone and tooth.

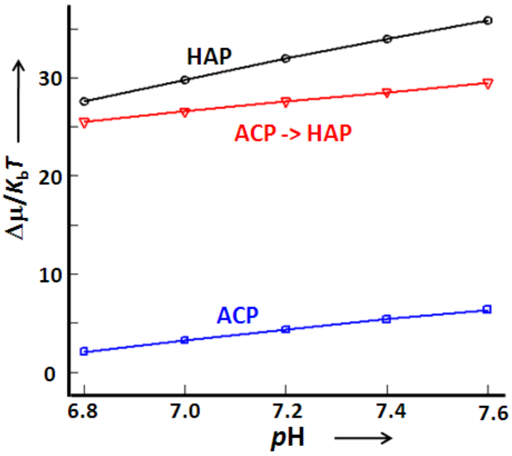

Figure S3. Chemical potentials of calcium phosphate solutions under different pH conditions.

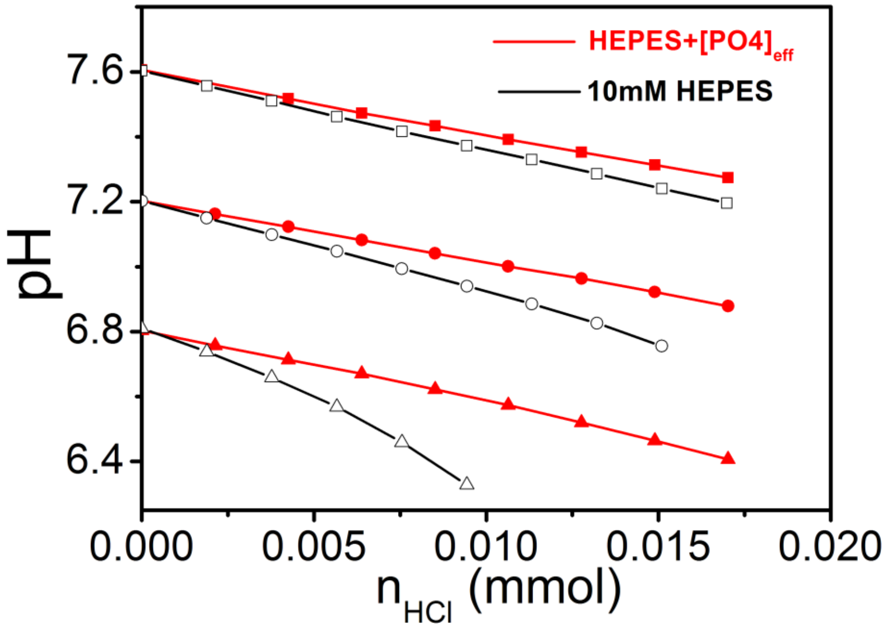

Figure S4. Titration curves of HEPES-phosphate andHEPES solutions under different initial *p*H conditions. Ten mL of buffer solutions were titrated with 0.5M HCl. The *p*H drops faster at lower *p*H conditions. When phosphate is removed from system, the buffer capacity is reduced as well, which can explain the faster drop of *p*H as HAP formation (Fig. 1).